Domain gain or loss in fungal chitinases drives ecological specialization toward antagonism or immune suppression

Ruben Eichfeld[1,2], Asmamaw B. Endeshaw[1], Margareta J. Hellmann[3], Bruno M. Moerschbacher[3], Alga Zuccaro[1,2*]

[1]University of Cologne, Institute for Plant Sciences, Cologne, Germany

[2]Cluster of Excellence on Plant Sciences (CEPLAS), Cologne, Germany

[3]University of Münster, Institute of Biology and Biotechnology of Plants, Münster, Germany

*Correspondence: azuccaro@uni-koeln.de

Abstract

The evolutionary origins of fungal effector proteins remain poorly understood, particularly how structural changes reprogram antimicrobial enzymes into host-adapted immune suppressors. Here, we show that domain modularity drives ecological specialization in chitinase effectors of the beneficial root endophyte *Serendipita indica*. The GH18 chitinase *Si*CHIT, which carries a C-terminal carbohydrate-binding module (CBM5), is expressed during fungal competition and antagonizes the fungal pathogen *Bipolaris sorokiniana* in the rhizosphere, thereby protecting plant roots. Deletion of the CBM5 abolishes this antifungal activity, while fusion of CBM5 to the CBM5-lacking paralog *Si*CHIT2 restores pathogen inhibition. In contrast, *Si*CHIT2 is induced during root colonization and suppresses chitin-triggered reactive oxygen species production, promoting immune evasion and host compatibility. These results identify CBM5 as a modular determinant of effector function, switching chitinase activity between microbial antagonism and host immune suppression. Our findings support an evolutionary scenario

in which effector function in planta arises through domain loss and transcriptional divergence from an antimicrobial precursor, consistent with transitions along the saprotrophy-to-symbiosis continuum.

Significance Statement

Effector proteins play key roles in shaping fungal interactions with both plant hosts and microbial competitors, yet how these functions evolve remains unclear. Here, we show that structural domain modularity enables ecological specialization of two paralogous chitinases arising from gene duplication in the root endophyte *Serendipita indica*. Through domain deletion and fusion, we demonstrate that a carbohydrate-binding module (CBM5) determines whether a chitinase functions in microbial antagonism or immune evasion. Our findings provide mechanistic evidence for effector diversification via domain loss and transcriptional divergence, supporting an evolutionary trajectory from antimicrobial activity to host adaptation. This work advances our understanding of how modular architecture drives effector evolution and niche specialization in symbiotic fungi.

Highlights

- Gain or loss of a CBM5 binding domain drives effector specialization between fungal antagonism and immune suppression
- CBM5 acts as a modular determinant enabling antifungal activity in the GH18 chitinase *Si*CHIT
- The CBM5-lacking paralog *Si*CHIT2 suppresses host immunity and promotes root colonization
- Functional divergence following gene duplication illustrates evolutionary repurposing of an antimicrobial enzyme into an immune-suppressive effector

Introduction

Mutualistic fungi are ecologically important members of the rhizosphere microbiome, where they support plant health and influence microbial community structure and function (Martin & Tan, 2025) This diverse group includes ectomycorrhizal and arbuscular mycorrhizal fungi, as well as beneficial root endophytes. Unlike mycorrhizal fungi, root endophytes often colonize plant roots without forming specialized symbiotic structures and, depending on the host and environmental context, can enhance plant performance by promoting nutrient uptake, water acquisition, and tolerance to environmental stress (Vandenkoornhuyse *et al.*, 2002; Dastogeer *et al.*, 2018; Mesny *et al.*, 2021; Mahdi *et al.*, 2022; Andreo-Jimenez *et al.*, 2023; Zhang *et al.*, 2024). These fungi exemplify the evolutionary plasticity of fungal lifestyles, flexibly occupying ecological niches along the saprotrophy-to-symbiosis continuum. To colonize plant roots and shape their ecological niche, beneficial root endophytes must overcome two key challenges: evasion of host immunity and competition with microbial antagonists and plant pathogens, a process recently shown to be supported by synergistic interactions with bacterial members of the core microbiota (Mahdi *et al.*, 2022). Both immune evasion and microbial competition are mediated by secreted effector proteins. Effector-mediated immune evasion often involves the degradation or masking of microbe-associated molecular patterns (MAMPs), such as β-1,6-glucan and chitin, to prevent recognition by host pattern recognition receptors (Lahrmann & Zuccaro, 2012; Fesel & Zuccaro, 2016; Wawra *et al.*, 2016). In parallel, effectors can alter the microbiota composition by suppressing microbial competitors, a strategy well documented in plant pathogens (Snelders *et al.*, 2020; Snelders *et al.*, 2021) and increasingly recognized in mutualistic fungi.

The beneficial root endophyte *Serendipita indica* (*Si*), a member of the widespread fungal order Sebacinales (Basidiomycota), colonizes a broad range of host plants and is known for its ability to promote growth and suppress plant immunity while protecting the host from pathogens. Colonization is confined to the rhizoplane, epidermis, and cortex, and depends on an intact host immune system (Lahrmann *et al.*, 2015). In addition to its host-associated functions, *Si* exhibits strong antifungal activity in the rhizosphere, particularly against the pathogen *Bipolaris sorokiniana (Bs)*, the causal agent of spot blotch and root

rot in cereals (Sarkar *et al.*, 2019; Mahdi *et al.*, 2022; Eichfeld *et al.*, 2024). This antagonism is mediated by a GH18-CBM5 endochitinase (*Si*CHIT), whose catalytic activity restricts *Bs* growth and recapitulates *the* protective effect of *Si* in planta (Eichfeld *et al.*, 2024).

GH18 chitinases, found across all fungal phyla, cleave β-1,4-glycosidic bonds in chitin, a major structural component of fungal cell walls. These enzymes fulfill diverse roles in nutrient scavenging, hyphal remodeling, and fungal antagonism (Seidl, 2008; Chen *et al.*, 2020). Their catalytic activity depends on a conserved DxxDxDxE motif, which defines the substrate-assisted catalytic mechanism characteristic of this family (van Aalten *et al.*, 2001; Bußwinkel *et al.*, 2018). While some chitinase-derived effectors have lost enzymatic activity and evolved to sequester MAMPs (Fiorin *et al.*, 2018), others retain catalytic function and are functionally enhanced by accessory domains such as carbohydrate-binding modules (CBMs) (Limón *et al.*, 2001; Limón *et al.*, 2004; Monge *et al.*, 2018). These non-catalytic domains increase substrate affinity and specificity, particularly for crystalline or polymeric forms of chitin (Itoh *et al.*, 2006; Matroodi *et al.*, 2013). *Si*CHIT features a C-terminal CBM5 domain, a modular architecture found predominantly in bacteria and Basidiomycota but absent in Ascomycota, suggesting a lineage-specific evolutionary adaptation (Chen *et al.*, 2020; Eichfeld *et al.*, 2024). Here, we investigate the functional significance of CBM5 in *Si*CHIT and examine how domain architecture modulates effector activity, enabling a switch between microbial antagonism and immune evasion.

We show that the CBM5 domain is essential for the antifungal and plant-protective function of *Si*CHIT. This chitinase is expressed during fungal competition and antagonizes the pathogen *Bs* in the rhizosphere, thereby protecting plant roots. In contrast, its closely related paralog *Si*CHIT2 lacks CBM5 and is induced during root colonization. *Si*CHIT2 promotes evasion of chitin-triggered immunity, preventing the generation of host-derived reactive oxygen species. Through domain-swapping experiments, we demonstrate that CBM5 functions as a modular determinant that switches the ecological role of a chitinase from microbial antagonism to host immune suppression. Together, our findings support a model in which effector specialization emerges through gene duplication, domain loss,

110 and transcriptional divergence, reprogramming an antimicrobial enzyme into a host-
111 adapted immune effector.

112 Results

113 CBM5 enhances binding to crystalline chitin and fungal cell wall without altering product specificity

114 To investigate the role of the C-terminal CBM5 domain in *Si*CHIT (PIIN_03543), we
115 generated three recombinant variants: full-length *Si*CHIT, a catalytically inactive mutant
116 (*Si*CHIT^{E196Q}), and a truncated version lacking the CBM5 domain (*Si*CHIT^{-CBM5}), which
117 retained the proline-rich linker. The truncated construct was produced by excluding the
118 final 141 bp from the coding sequence. All recombinant proteins were purified via affinity
119 chromatography and verified by SDS-PAGE (Fig. S1).

120 We first assessed chitinase activity on insoluble crab shell chitin using thin-layer
121 chromatography (TLC) and by quantifying reducing sugars after 20 hours of incubation
122 (Fig. 1A, B). These assays, along with endpoint measurements on chitin azure (CA) (Fig.
123 1C), revealed no major differences between full-length *Si*CHIT and *Si*CHIT^{-CBM5}.
124 However, time-course experiments on CA showed that the presence of CBM5 enhanced
125 early hydrolysis (Fig. 1D), suggesting that the domain increases the reaction rate during
126 initial substrate engagement.

127 To evaluate whether CBM5 influences product outcome, we analyzed the hydrolysates of
128 colloidal chitin by mass spectrometry. Both *Si*CHIT and *Si*CHIT^{-CBM5} produced similar
129 oligomer profiles dominated by chitobiose (A2), indicating that CBM5 does not alter
130 product specificity (Fig. 1E). Notably, substantial amounts of partially deacetylated
131 products, such as A1D1 and A2D2, were also detected. This likely reflects the fact that
132 colloidal chitin is not fully acetylated; deacetylated regions may form stretches with higher
133 solubility and increased accessibility, leading to their preferential cleavage by the
134 enzymes. To assess whether CBM5 affects subsite preferences, we analyzed the
135 hydrolysis products of chitosans with defined degrees of acetylation (DA). *Si*CHIT^{-CBM5}
136 displayed the same requirement for an acetylated unit at the -1 subsite and no detectable
137 shifts at adjacent positions compared to *Si*CHIT, confirming that CBM5 does not influence
138 catalytic specificity (Fig. 1F; Eichfeld *et al*., 2024).

139 To determine the role of CBM5 in substrate interaction, we performed pull-down assays
140 using crab shell chitin, highly deacetylated chitosan, and lyophilized, protein-free *Bs*
141 mycelium. *Si*CHIT^{-CBM5} showed reduced binding to crab shell chitin compared to full-
142 length *Si*CHIT, while no difference was observed with chitosan, suggesting that CBM5
143 enhances binding specifically to acetylated, crystalline substrates (Fig. 1G). Binding to *Bs*
144 mycelium was also reduced in the absence of CBM5, indicating that the domain
145 contributes to cell wall targeting.

146 Together, these results show that while CBM5 is dispensable for full catalytic activity and
147 does not alter product specificity, it enhances early hydrolysis rates and substrate binding,
148 particularly to crystalline or fungal cell wall-like chitin. This suggests that CBM5 improves
149 functional efficiency under biologically relevant conditions, likely contributing to the
150 ecological role of *Si*CHIT in microbial competition.

151 CBM5 is required for antifungal activity and plant protection

152 We previously demonstrated that *Si*CHIT restricts the growth of *Bs* and reduces its
153 colonization of plant roots through its chitinolytic activity (Eichfeld *et al*., 2024). However,
154 the specific contribution of the CBM5 domain to this antifungal function remained
155 unresolved. To test whether CBM5 is required for *Bs* inhibition, we incubated *Bs* spores
156 with the full-length *Si*CHIT, the catalytically inactive mutant *Si*CHIT^{E196Q}, the truncated
157 variant lacking CBM5 *Si*CHIT^{-CBM5}, or the empty vector control Ev. As expected, *Bs* spore
158 germination was significantly reduced in the presence of active *Si*CHIT, but not with
159 *Si*CHIT^{E196Q}. *Si*CHIT^{-CBM5} showed a similar lack of inhibitory effect as *Si*CHIT^{E196Q} and
160 had only a minimal effect compared to the Ev control (Fig. 2A).

161 We next examined whether the loss of antifungal activity translates into reduced
162 protection of host roots. *Bs* spores treated with the same chitinase variants were used to
163 inoculate the roots of the *Bs* host *Hordeum vulgare* (*Hv*). As previously shown, *Si*CHIT-
164 treated spores led to a significant reduction in *Bs* colonization, as measured by fungal
165 transcript levels in roots. In contrast, *Si*CHIT^{E196Q} and *Si*CHIT^{-CBM5} had no effect (Fig. 2B).
166 Correspondingly, only *Si*CHIT mitigated the reduction in root biomass caused by *Bs*
167 infection (Fig. 2C). To test whether this effect is conserved in other hosts, we repeated

168 the experiment using *Arabidopsis thaliana* (*At*). *Si*CHIT reduced *Bs* biomass and
169 preserved root elongation, while *Si*CHIT^{E196Q} did not. *Si*CHIT^{-CBM5} had a weak protective
170 effect, albeit significantly lower than the full-length enzyme. (Fig. S2.).

171 Together, these results demonstrate that both chitinase activity and the CBM5 domain are
172 required for *Si*CHIT's antifungal and plant-protective functions. The loss of protection
173 observed in the CBM5-lacking variant suggests that this domain contributes to cell wall
174 binding and is critical for effective niche defense.

175 A CBM5-lacking paralog, *Si*CHIT2, is transcriptionally specialized for host colonization

176 GH18-CBM5 chitinases are absent in Ascomycota but occur frequently in the
177 Agaricomycetes (Basidiomycota), where gene copy number varies across species with
178 different ecological lifestyles (Eichfeld et al., 2024). To better define the structural
179 requirements for antifungal activity in *Si*, we compared the four GH18 chitinases encoded
180 in the genome with respect to phylogenetic relationships, domain architecture, and
181 transcriptional regulation. Of the four, only *Si*CHIT harbors a CBM5 domain, whereas the
182 other three chitinases contain no additional domains besides the GH18 catalytic domain
183 (Fig. 3A). *Si*CHIT and its closest paralog *Si*CHIT2 (PIIN_03542) share the highest
184 sequence identity and form a distinct phylogenetic pair among the *Si* GH18 chitinases
185 (Fig. 3A; Supplementary Fig. S3). The catalytic DxxDxDxE motif located at the -1 subsite
186 is conserved across all four chitinases, suggesting that each is catalytically active (Fig.
187 3B). Despite this shared motif, the chitinases exhibit distinct structural features. *Si*CHIT2
188 retains an 86-amino-acid C-terminal linker but lacks a CBM5 domain. *Si*CHIT3
189 (PIIN_11727) lacks a predicted signal peptide, while *Si*CHIT4 (PIIN_07603), features
190 extended surface-exposed loops within the GH18 domain (Supplementary Table S1).
191 Taken together, *Si*CHIT and *Si*CHIT2 are more similar to each other in sequence,
192 structure, and genomic context than to the other chitinases in *Si*. Notably, they are located
193 adjacent in the genome (Fig. 3C). Their tandem organization, high sequence identity, and
194 absence of CBM5 in *Si*CHIT2 support a gene duplication event followed by structural
195 divergence through domain loss.

196 To assess structural similarity, we generated AlphaFold models of both enzymes after
197 removing the predicted signal peptides. The models confirmed the overall structural
198 conservation of the GH18 catalytic domain and the presence of a C-terminal linker in
199 *Si*CHIT2, but no CBM5 domain (Fig. 3D & E)

200 To examine transcriptional regulation, we analyzed RNA-seq data from Eichfeld et al.
201 2024 and found that *Si*CHIT and *Si*CHIT2 were the only chitinases significantly
202 upregulated in biotic contexts. *Si*CHIT was specifically induced during fungal
203 confrontation, while *Si*CHIT2 was induced during colonization of barley, *Brachypodium*
204 and *Arabidopsis*. In contrast, *Si*CHIT3 and *Si*CHIT4 were not transcriptionally activated
205 under any tested biotic conditions, including interactions with pathogenic fungi, beneficial
206 bacteria, or different plant hosts (Fig. 3F & G). To extend the RNA-seq findings, we
207 measured the expression of *Si*CHIT and *Si*CHIT2 by qPCR following confrontation with
208 *Bs* and six additional filamentous fungi representing the major fungal lineages
209 Ascomycota, Basidiomycota, and Mucoromycota. *Si*CHIT was induced in several of these
210 interactions, whereas *Si*CHIT2 expression remained low under all tested microbial
211 conditions (Fig. 3H). Additionally, both *Si*CHIT and *Si*CHIT2 were induced when *S. indica*
212 was grown on crab shell chitin as the sole carbon source (Fig. 3I).

213 Together, these findings suggest that *Si*CHIT2 evolved a distinct ecological function from
214 *Si*CHIT following gene duplication. Their divergent domain architecture and expression
215 profiles indicate functional specialization, with *Si*CHIT adapted for fungal antagonism and
216 *Si*CHIT2 for host colonization.

217 Fusion of CBM5 reprograms *Si*CHIT2 for fungal antagonism

218 To test whether the CBM5 domain of *Si*CHIT is sufficient to confer antifungal activity, we
219 constructed a chimeric protein consisting of the GH18 catalytic domain of *Si*CHIT2 fused
220 to the proline-rich linker and CBM5 domain of *Si*CHIT (*Si*CHIT2^{+CBM5}). As a control, we
221 generated a second construct in which only the linker was fused to the GH18 domain of
222 *Si*CHIT2 (*Si*CHIT2^{+link}) (Fig. 4A). As observed for native *Si*CHIT and *Si*CHIT^{-CBM5}, the
223 presence of CBM5 did not affect endpoint chitinase activity on crab shell chitin or chitin
224 azure (Fig. 4B, C). However, only *Si*CHIT2^{+CBM5} suppressed *Bs* spore germination,

225 comparable to the effect of full-length *Si*CHIT. In contrast, *Si*CHIT2^{+link} showed no
226 inhibitory activity (Fig. 4D). Consistent with these results, both *Si*CHIT and *Si*CHIT2^{+CBM5}
227 reduced root growth inhibition in barley caused by *Bs*, and limited pathogen colonization.
228 In contrast, *Si*CHIT^{-CBM5} and *Si*CHIT2^{+link} had no measurable protective effect (Fig. 4E &
229 F).

230 These results demonstrate that fusing CBM5 to *Si*CHIT2 is sufficient to confer antifungal
231 activity, indicating that CBM5 acts as a modular domain enabling functional adaptation
232 toward microbial antagonism.

233 *Si*CHIT2 suppresses chitin-triggered immunity and facilitates root colonization by *S. indica*

234 Given the distinct plant-induced expression profile of *Si*CHIT2, we hypothesized that this
235 chitinase contributes to immune evasion during root colonization. Previous studies have
236 shown that *Podosphaera xanthii* uses chitinase-like effectors to degrade immunogenic
237 chitin oligomers and suppress host defense responses (Martínez-Cruz *et al.*, 2021). To
238 test whether *Si* chitinases function similarly, we incubated immunogenic chitohexaose
239 (A6) with recombinant *Si*CHIT, *Si*CHIT2, their respective variants, or the Ev control at a
240 1:1 molar ratio. The resulting hydrolysates were applied to barley roots to measure
241 reactive oxygen species (ROS) production. ROS accumulation was completely abolished
242 when chitohexaose was pre-treated with either *Si*CHIT2^{+link} or *Si*CHIT^{-CBM5}. In contrast,
243 treatment with *Si*CHIT2^{+CBM5} or full-length *Si*CHIT resulted in only partial or no
244 suppression of ROS accumulation (Fig. 5A, B). An intermediate reduction in ROS
245 accumulation was observed when chitohexaose was pre-treated with *Si*CHIT^{E196Q}, likely
246 due to the inactive catalytic cleft sequestering a fraction of the chitohexaose. None of the
247 recombinant chitinases induced ROS when applied in the absence of chitohexaose (Fig.
248 S4).

249 To assess whether this immune suppression contributes to host colonization, we co-
250 inoculated *Si* with 20 μM of each recombinant chitinase and quantified fungal biomass in
251 barley roots at three days post-inoculation. *Si*CHIT2^{+link} significantly enhanced root
252 colonization, whereas the other chitinases did not (Fig. 5C). *Si*CHIT^{-CBM5} showed a slight
253 but non-significant trend toward increased colonization.

254 These results suggest that *Si*CHIT2's ability to suppress ROS depends on the absence
255 of CBM5, which may otherwise restrict access to soluble substrates and favor binding to
256 insoluble chitin. This immune-suppressive function, together with its host-specific
257 transcriptional induction, underscores a distinct ecological role for SiCHIT2 compared to
258 its CBM5-containing paralog.

259 Discussion

260 Effector proteins are central to the ecological success of root-colonizing fungi, mediating
261 interactions not only with host plants but also with competing microbes. While traditionally
262 associated with immune suppression (Stergiopoulos & de Wit, 2009), fungal effectors are
263 now also recognized for their roles in inter-microbial competition. They facilitate the
264 acquisition and maintenance of ecological niches in the rhizosphere and on root surfaces,
265 thereby supporting fungal persistence and competitive advantage (Snelders *et al.*, 2020;
266 Gómez-Pérez *et al.*, 2023; Eichfeld *et al.*, 2024). These dual roles are not restricted to
267 pathogens; beneficial fungi such as *Si* employ similar strategies to persist in complex
268 microbial communities, maintain host compatibility, and defend their ecological niche.
269 This functional versatility reflects broader evolutionary trends across the fungal kingdom,
270 where transitions from saprotrophy to symbiosis are accompanied by the repurposing of
271 ancestral traits to meet ecological demands.

272 Here, we show that *Si* encodes two closely related GH18 chitinases, *Si*CHIT and
273 *Si*CHIT2, that have diverged structurally and transcriptionally to perform distinct
274 ecological functions. *Si*CHIT, which carries a C-terminal CBM5 domain, is expressed
275 during fungal confrontation and contributes to pathogen growth inhibition and plant
276 protection. In contrast, *Si*CHIT2, is induced during root colonization, and suppresses
277 chitin-triggered immune responses in the host (Fig. 5). This divergence possibly reflects
278 an evolutionary trajectory driven by gene duplication and domain loss, enabling *Si* to
279 balance microbial antagonism and host compatibility through modular effector
280 specialization.

281 The importance of domain modularity in effector function is supported by previous studies
282 in *Trichoderma* spp., where the addition of substrate-binding domains such as CBM1 or

283 CBM18 increases their binding affinity for insoluble substrates and enhances antifungal
284 activity by improving proximity and substrate targeting (Limón *et al.*, 2001; Limón *et al.*,
285 2004). However, such effects can be masked in vivo by genome-wide redundancy in cell
286 wall-degrading enzymes and antimicrobial effectors. Using purified proteins, we
287 demonstrate that the CBM5 domain is critical for the antifungal activity of *Si*CHIT. Its
288 deletion abolishes fungal antagonism and its reintroduction into *Si*CHIT2 restores this
289 function. This is consistent with studies in bacterial chitinases, where CBM5 loss reduces
290 antifungal activity, likely due to impaired substrate binding (Tsujibo *et al.*, 2003; Itoh *et al.*,
291 2006). In our assays, CBM5 enhanced early hydrolysis rates and binding to crystalline
292 chitin and fungal cell wall, but did not affect overall catalytic activity or product profile. This
293 suggests a proximity-based enhancement mechanism, in which CBM5 anchors the
294 enzyme at the fungal cell wall. Unlike antimicrobial or agglutinating lectins such as WSC3,
295 a β-1,3-glucan-binding lectin from *S. indica* that agglutinates fungal cells independently
296 of enzymatic activity (Wawra *et al.*, 2019), CBM5 alone does not provide antifungal activity
297 which requires a catalytically active GH18 core. Some fungal pathogens employ
298 catalytically inactive chitinase effectors (e.g., *Mp*Chi in *Moniliophthora perniciosa*; Fiorin
299 *et al.*, 2018) or active chitinases (e.g., *Mo*Chia1 in *Magnaporthe oryzae*; Yang & Yu, 2019;
300 Martínez-Cruz *et al.*, 2021), or EWCAs; Martínez-Cruz *et al.*, 2021) to suppress host
301 immunity by sequestering or degrading free chitin oligomers. Similarly, we show that both
302 *Si*CHIT2 and *Si*CHIT^{-CBM5} can suppress chitohexaose-induced ROS production. These
303 findings suggest that CBM5 may hinder activity on soluble substrates not by altering
304 catalytic specificity, but by limiting access to short oligomers through spatial constraints.
305 CBM5 domains are structurally optimized for engaging extended, crystalline chitin
306 surfaces via aromatic stacking and hydrogen bonding (Kezuka *et al.*, 2006; Vaaje-Kolstad
307 *et al.*, 2019). Accordingly, CBM5-containing chitinases like *Si*CHIT likely localize to
308 insoluble polysaccharides in fungal cell walls, anchoring the enzyme to non-immunogenic
309 material. Although such substrate targeting could in principle restrict access to soluble
310 MAMPs, this is unlikely in the ROS assay, where only chitohexaose is present. A more
311 plausible explanation is that CBM5 increases the rigidity or steric bulk of the protein,
312 thereby reducing flexibility and limiting productive interaction with short ligands. In
313 contrast, CBM5-lacking variants such as *Si*CHIT2 remain free to access and degrade free

314 immunogenic chitin oligomers. This suggests that suppression of host immunity may
315 require a CBM5-free configuration optimized for apoplastic MAMP degradation during
316 root colonization. Such structural neofunctionalization provides a plausible trajectory for
317 the evolution of fungal effector functions. Given the saprotrophic ancestry and facultative
318 symbiotic lifestyle of *S. indica*, *Si*CHIT likely evolved under selective pressure from fungal
319 competitors, whereas *Si*CHIT2 emerged as an immune-suppressive effector during the
320 transition to a root-associated niche. This represents a clear case of functional divergence
321 driven by domain loss and regulatory rewiring. By comparison, the *Verticillium dahliae*
322 effector *Vd*AMP3 illustrates a different evolutionary strategy: co-opted from an ancestral
323 antimicrobial protein, it retains both its antimicrobial activity and core structural features
324 while functioning in microbiota manipulation in planta. Rather than undergoing major
325 neofunctionalization, *Vd*AMP3 shows how effectors can be repurposed for new ecological
326 roles with minimal structural change (Snelders *et al.*, 2021). This highlights the diversity
327 of evolutionary pathways by which fungal effectors adapt to changing environments.

328 Together, our findings show that domain gain and loss can reprogram effector proteins for
329 distinct ecological roles. CBM5 serves as a modular determinant, switching GH18
330 chitinase activity between microbial antagonism and immune suppression. This highlights
331 how structural modularity enables fungi to adapt effectors to the dual pressures of
332 rhizosphere competition and host interaction in symbiotic fungi.

333 Material and Methods

334 Plant and fungal materials

335 *Hordeum vulgare* (*Hv*, L. cv Golden Promise) and *Arabidopsis thaliana* (*At*, Col-0) were
336 used as plant hosts. *Hv* seeds were surface-sterilized in 6 % sodium hypochlorite for 1 h
337 under constant shaking and subsequently washed five times for 30 min in sterile water.
338 Seeds were germinated for four days on wet filter paper at 21 °C in the dark. Seeds of *At*
339 were surface-sterilized in 70 % ethanol for 10 min and 100 % ethanol for 7 min. *At* seeds
340 were placed on ½ MS medium (Murashige-Skoog medium including vitamins, pH 5.6)
341 containing 1 % sucrose and stratified for three days in the dark prior to germination on a
342 day-night cycle of 8/16 h at 22/18 °C, 60 % humidity and 125 µmol/m^2 light intensity for

343 seven days. *Serendipita indica* (*Si*, DSM11827) and *Bipolaris sorokiniana* (*Bs*, ND90Pr)
344 were used as fungal species. *Si* was grown on CM medium (Complete Medium, 1.5 %
345 agar) at 28 °C for 30 days in the dark. *Si* spores were harvested by adding sterile water
346 and scraping the spores with a scalpel. The suspension was filtered through a sterile
347 miracloth filter and spores were centrifuged at 2,000 x g. The supernatant was discarded
348 and spores were washed three times in water. *Bs* was grown on modified CM medium
349 (Sarkar *et al.*, 2019) at 28 °C for 14 days in the dark. *Bs* spores were harvested like *Si*
350 spores but a Drigalski spatula was used to scrape the spores instead of a scalpel.

351 Preparation of fungal inoculants and plant colonization

352 For the preparation of *Bs* inoculants, spores were harvested from 21-day old plates and
353 incubated with the respective recombinant proteins (10 µM in 50 mM phosphate buffer)
354 for 16 h at 28 °C in the dark. Spore mixtures were diluted to 5000 spores/mL to yield the
355 final working inoculants. For inoculation of *At*, ten sterile seven-day old seedlings were
356 placed on solid 1/10 PNM (pH 5.6) plates (0.005 % KNO_3, 0.005 % KH_2PO_4, 0.0025 %
357 K_2HPO_4, 0.049 % $MgSO_4$, 0.00472 % $Ca(NO_3)_2$, 0.0025 % NaCl, 0.5 % (v/v) Fe-EDTA
358 stock solution, 1.2 % Gelrite, pH 5.6. After autoclaving, 10 mL 1 M MES pH 5.6 was
359 added. The EDTA stock solution contains 2.78 % $FeSO_4$ x 7 H_2O, 4.13 % Na_2EDTA x
360 $2H_2O$. Concentrations are indicated in w/v if not stated otherwise) and the roots were
361 treated with 1 mL of the respective inoculant. The root elongation was quantified by
362 measuring the difference root length at the start of the inoculation and the end of the
363 experiment at three days post inoculation (dpi). Roots were washed with water and snap
364 frozen in liquid nitrogen for further RNA extraction. For inoculation of *Hv*, four sterile
365 seedlings were placed in glass jars containing solid 1/10 PNM medium (pH 5.6) and
366 inoculated with three mL of the respective inoculant. The root weight was quantified at
367 three dpi. Roots were washed in water and snap frozen for further RNA extraction. For
368 the preparation of *Si* inoculants, spores were harvested from 28-day old plates and were
369 allowed to germinate overnight in sterile water at 28 °C. Prior to plant root inoculation, the
370 respective recombinant proteins were added to 20 µM in 50 mM phosphate buffer.
371 Subsequently, the roots of four day-old *Hv* seedlings were inoculated with three mL of

372 500,000 spores/mL. *Hv* seedlings were harvested at three dpi, washed in water and snap
373 frozen in liquid nitrogen.

374 Preparation of fungal confrontations

375 For the preparation of fungal inoculants, liquid CM medium was inoculated with 500,000
376 spores/mL. For all other fungi, mycelium was scraped from plates and transferred to liquid
377 CM. All fungi were grown for six days at 28 °C and 120 rpm. The mycelium was blended
378 and re-suspended in fresh CM and regenerated for another 24 h. Regenerated mycelium
379 was filtered through miracloth filters and washed thoroughly with sterile milliQ water.
380 Fungal mycelia were mixed in a 1:1 ratio and 1 g of mycelium was streaked on PNM
381 plates containing 15 % agar. After six days, the mycelia were harvested, dried with tissue
382 papers and snap frozen in liquid nitrogen.

383 Fungal spore germination

384 To quantify the *Bs* spore germination, isolated spores were resolved in liquid CM to a
385 concentration of 100,000 spores/mL and 100 µL were added to the wells of sterile Lab-
386 Tek 2 chamber slides with cover (VWR). 100 µL of the respective treatment (Ev control or
387 purified protein) were added to a final concentration of 10 µM. The germination rate of
388 spores was quantified 6 h after treatment.

389 RNA extraction from plant roots and RT-qPCR

390 Plant materials were ground in liquid nitrogen and 1 mL of TRIzol reagent (Thermo
391 Fischer scientific) was added. Samples were vortexed for 20 sec until all material was
392 resolved. 200 µL chloroform were added and samples vortexed again. Samples were
393 centrifuged at 17,000 x g and 4 °C for 30 min and 500 µL of the upper aqueous phase
394 were transferred to 500 µL isopropanol. The nucleic acids were precipitated at -20 °C for
395 16 h and pelleted by centrifugation at 17,000 x g and 4 °C for 30 min. Pellets were
396 washed three times with 70 % ethanol diluted in DEPC water. Remaining DNA was
397 removed by adding 1 µL DNase1 (1 U/µL) in 3 µL DNase1 buffer (10 x) (Thermo Fischer
398 scientific) and 26 µL RNase-free water. Samples were incubated at 37 °C for 30 min.
399 DNase digest was stopped by heating to 70 °C for 5 min and subsequent precipitation
400 with 2 volumes isopropanol and ½ volume of 7.5 M ammonium acetate for 16 h at -20 °C.
401 Samples were washed twice with 70 % ethanol in DEPC water and resolved in 30 µL

402 RNase-free water. Concentrations were determined using a NanoDrop 2000c
403 spectrophotometer (Thermo Fischer Scientific).

404 1 µg of RNA was used for reverse transcription into cDNA (Thermo Fischer Scientific).
405 First, 1 µL of random hexamer and of oligo-dt oligomers were added and incubated at
406 65 °C for 5 min and subsequently placed on ice. 4 µL 5 x reaction buffer, 1 µL Riboblock
407 RNase inhibitor (20 U/µL), 2 µL 10 mM dNTPs and 2 µL MMLV reverse transcriptase were
408 added and samples were incubated at 42 °C for 1 h. cDNA synthesis was stopped by
409 heating to 70 °C for 5 min. RT-qPCR was conducted using the primers listed in
410 Supplementary Table S2.

411 Cloning of chitinase expression vectors

412 The coding sequence (CDS) of the chitinase genes were amplified by PCR with Q5 High-
413 Fidelity Polymerase (New England Biolabs) using the primers listed in Supplementary
414 Table S2. PCR products were cloned using the Gibson assembly cloning technique into
415 the PQE80L expression vector (Qiagen, Hilden, Germany) after vector linearization with
416 Kpn1 (New England Biolabs).

417 Production and purification of recombinant protein in *E. coli*

418 Chemically competent *E. coli* BL21 cells were transformed with the vectors for protein
419 expression under control of a lac operon. 5 mL starter cultures were prepared in liquid LB
420 medium containing 100 µg/mL carbenicillin and grown for 16 h at 37 °C and 180 rpm.
421 Starter cultures were transferred to 300 mL of LB medium with carbenicillin and grown to
422 an OD_{600} of 0.5 at 28 °C. Gene expression was induced by adding IPTG to a final
423 concentration of 1 mM and cells were grown at 16 °C for 20 h. Cells were pelleted by
424 centrifugation at 5000 g for 15 min at 4 °C. Bacterial pellets were resolved in 5 mL lysis
425 buffer (50 mM NaH_2PO_4, 300 mM NaCl and 10 mM imidazole, pH 8) and sonicated three
426 times for 1 min with pulses on ice and centrifuged at 16,200 g for 30 min. 5 mL of the
427 supernatant were added to 1 mL of Nickel-NTA Agarose (Qiagen, Hilden, Germany) and
428 incubated under continuous shaking at 4 °C for 1 h. Samples were spun down at 500 g
429 for 10 secs, the flow through was removed, 4 mL wash buffer (50 mM NaH_2PO_4, 300 mM
430 NaCl and 20 mM imidazole, pH 8) were added and samples were incubated under

431 continuous shaking at 4 °C for 10 min. Washing steps were repeated five times. For
432 elution, 1 mL of elution buffer (50 mM NaH_2PO_4, 300 mM NaCl and 250 mM imidazole,
433 pH 8) was added and samples were incubated under continuous shaking at 4 °C for 10
434 min. Eluted fractions were dialyzed against 50 mM phosphate buffer (pH 6) over night
435 and protein concentrations were measured using Bradford reagent. To test the purity of
436 the protein samples, aliquots were boiled for 5 min in SDS-sample buffer, loaded on a 10
437 % SDS gel and visualized by Coomassie staining.

438 Chitinase activity assays

439 To quantify the enzymatic activity of the purified chitinases, 2 mg/mL chitin azure (Sigma
440 Aldrich) were incubated with 5 µM recombinant chitinase in a total volume of 200 µL.
441 Reactions were incubated at 28 °C for 20 h. Reactions were stopped by heating to 95 °C
442 for 5 min and samples were centrifuged 5 min at 17,000 x g and the absorbance of
443 supernatants was quantified at 560 nm. For quantifying reducing ends, 10 g crab shell
444 chitin were incubated with 5 µM enzyme in 200 µL 50 mM phosphate buffer for 20 h at
445 28 °C. Reactions were stopped by heating to 95 °C for 5 min. Samples were centrifuced
446 for 5 min at 17,000 x g and supernatant were mixed in a 1:1 ratio with DNSA (3,5-
447 dinitrosalicylic acid) reagent. DNSA reagent is prepared by mixing 1 % (w/v) 3,5-
448 dinitroslicylic acid, 1.6 % (w/v) sodium hydroxide, 30 % (w/v) potassium sodium tartrate
449 tetrahydrate. The samples were heated for 10 min at 95 °C and subsequently transferred
450 to ice. The absorbance of the samples was measured at 540 nm.

451 For TLC, 10 mg crab shell chitin (Sigma Aldrich) were weighed in 2 mL reaction tubes
452 and recombinant chitinases were added to a final concentration of 5 µM in 200 µL.
453 Reactions were incubated at 28 °C for 20 h and stopped by heating to 95 °C for 5 min.
454 Samples were centrifuged at 17,000 x g for 5 min. 10 µL of the supernatant were
455 separated on 60 F_{254} TLC (Sigma Aldrich) silica gel plates with running buffer (n-
456 butanol/methanol/28 % ammonium hydroxide/water, 5/4/2/1). Plates were dried and then
457 bathed in developer solution (1.6 g diphenylamine/1.6 mL aniline/12 mL 85 % phosphoric
458 acid/80 mL acetone). TLC plates were developed in an incubation oven at 100 °C for 20
459 to 30 min.

460 Chitinase subsite specificity

461 The subsite specificity of *Si*CHIT^{-CBM5} was determined as previously reported (Cord-
462 Landwehr *et al.*, 2017; Eichfeld *et al.*, 2024).

463 Substrate binding assay

464 15 mg of crab shell chitin (Sigma Aldrich), Chitosan (Sigma Aldrich) or freeze-dried
465 mycelium of *Bs* were weighed in a 2 mL reaction tube and incubated with 400 µL chitin-
466 binding buffer (2 mM KH_2PO_4, 8 mM Na_2HPO_4, 2 mM KCL) and 100 µL of 20 µM
467 recombinant protein shaking at 4 °C for 1 h. Samples were centrifuged at 17,000 x g for
468 5 min and 60 µL of the supernatant were mixed with 60 µL Bradford reagent. Protein
469 amounts were quantified at 595 nm and compared to the input amount.

470 Quantification of reactive oxygen species (ROS)

471 For elicitor preparation, 10 µM of chitohexaose were incubated with 10 µM of recombinant
472 chitinase or the buffer control for 16 h at 28 °C. Reactions were stopped by heating to
473 95 °C for 5 min and chitohexaose was diluted to 250 nM.

474 Four root pieces (0.5 cm) of four-day old barley seedlings were transferred to each well
475 of a 96-well microtiter plate (white, flat bottom) containing 200 µL of 2.5 mM 2-(N-
476 morpholino)ethanesulfonic acid (MES) buffer, pH 5.6. The plate was incubated for 16 h at
477 21°C for recovery. The buffer was replaced with 100 µL 2.5 mM MES buffer containing
478 20 µM LO-12 and 20 µg/mL Horseradish peroxidase (HRP). After 25-min incubation in the
479 dark, 100 µL of 250 nM chitohexaose elicitor solution was added to each well.
480 Chemiluminescence was measured using a TECAN SPARK 10 M microplate reader over
481 all wells for 2 h with an integration time of 450 ms.

482 Data availability

483 All data supporting the findings of this study are available within the article and supporting
484 information.

Acknowledgements

We acknowledge support from the Cluster of Excellence on Plant Sciences (CEPLAS) funded by the Deutsche Forschungsgemeinschaft (DFG, German Research Foundation) under Germany's Excellence Strategy-EXC 2048/1-Project ID: 390686111 and the ZU 263/11-2 (SPP 2125 DECRyPT).

Competing interest

The authors declare no competing interest.

Author contributions

AZ and RE conceptualized the study. RE and AE conducted most of the research. MJH, BMM and RE conducted mass spectrometric analysis of the product profile and the subsite specificity. AZ and RE wrote the manuscript with input from all authors.

References

Andreo-Jimenez B, Te Beest DE, Kruijer W, Vannier N, Kadam NN, Melandri G, Jagadish SVK, van der Linden G, Ruyter-Spira C, Vandenkoornhuyse P, et al. 2023. Genetic Mapping of the Root Mycobiota in Rice and its Role in Drought Tolerance. *Rice (N Y)* **16**(1): 26.

Bußwinkel F, Goñi O, Cord-Landwehr S, O'Connell S, Moerschbacher BM. 2018. Endochitinase 1 (Tv-ECH1) from Trichoderma virens has high subsite specificities for acetylated units when acting on chitosans. *International Journal of Biological Macromolecules* **114**: 453-461.

Chen W, Jiang X, Yang Q. 2020. Glycoside hydrolase family 18 chitinases: The known and the unknown. *Biotechnology Advances* **43**: 107553.

Cord-Landwehr S, Ihmor P, Niehues A, Luftmann H, Moerschbacher BM. 2017. Quantitative Mass-Spectrometric Sequencing of Chitosan Oligomers Revealing Cleavage Sites of Chitosan Hydrolases. **89**(5): 2893-2900.

Dastogeer KMG, Li H, Sivasithamparam K, Jones MGK, Wylie SJ. 2018. Fungal endophytes and a virus confer drought tolerance to Nicotiana benthamiana plants through modulating osmolytes, antioxidant enzymes and expression of host drought responsive genes. *Environmental and Experimental Botany* **149**: 95-108.

Eichfeld R, Mahdi LK, De Quattro C, Armbruster L, Endeshaw AB, Miyauchi S, Hellmann MJ, Cord-Landwehr S, Peterson D, Singan V, et al. 2024. Transcriptomics reveal a mechanism of niche defense: two beneficial root endophytes deploy an antimicrobial GH18-CBM5 chitinase to protect their hosts. *New Phytologist* **244**(3): 980-996.

Fesel PH, Zuccaro A. 2016. β-glucan: Crucial component of the fungal cell wall and elusive MAMP in plants. *Fungal Genetics and Biology* **90**: 53-60.

521 **Fiorin GL, Sanchéz-Vallet A, Thomazella DPT, do Prado PFV, do Nascimento LC,**
522 **Figueira AVO, Thomma B, Pereira GAG, Teixeira P. 2018.** Suppression of Plant
523 Immunity by Fungal Chitinase-like Effectors. *Curr Biol* **28**(18): 3023-3030.e3025.
524 **Gómez-Pérez D, Schmid M, Chaudhry V, Hu Y, Velic A, Maček B, Ruhe J, Kemen A,**
525 **Kemen E. 2023.** Proteins released into the plant apoplast by the obligate parasitic
526 protist Albugo selectively repress phyllosphere-associated bacteria. *New*
527 *Phytologist* **239**(6): 2320-2334.
528 **Itoh Y, Watanabe J, Fukada H, Mizuno R, Kezuka Y, Nonaka T, Watanabe T. 2006.**
529 Importance of Trp59 and Trp60 in chitin-binding, hydrolytic, and antifungal
530 activities of Streptomyces griseus chitinase C. *Appl Microbiol Biotechnol* **72**(6):
531 1176-1184.
532 **Kezuka Y, Ohishi M, Itoh Y, Watanabe J, Mitsutomi M, Watanabe T, Nonaka T. 2006.**
533 Structural Studies of a Two-domain Chitinase from Streptomyces griseus
534 HUT6037. *Journal of Molecular Biology* **358**(2): 472-484.
535 **Lahrmann U, Strehmel N, Langen G, Frerigmann H, Leson L, Ding Y, Scheel D,**
536 **Herklotz S, Hilbert M, Zuccaro A. 2015.** Mutualistic root endophytism is not
537 associated with the reduction of saprotrophic traits and requires a
538 noncompromised plant innate immunity. *New Phytologist* **207**(3): 841-857.
539 **Lahrmann U, Zuccaro A. 2012.** Opprimo ergo sum--evasion and suppression in the root
540 endophytic fungus Piriformospora indica. *Mol Plant Microbe Interact* **25**(6): 727-
541 737.
542 **Limón MC, Chacón MR, Mejías R, Delgado-Jarana J, Rincón AM, Codón AC, Benítez**
543 **T. 2004.** Increased antifungal and chitinase specific activities of Trichoderma
544 harzianum CECT 2413 by addition of a cellulose binding domain. *Applied*
545 *Microbiology and Biotechnology* **64**(5): 675-685.
546 **Limón MC, Margolles-Clark E, Benítez T, Penttilä M. 2001.** Addition of substrate-
547 binding domains increases substrate-binding capacity and specific activity of a
548 chitinase from Trichoderma harzianum. *FEMS Microbiology Letters* **198**(1): 57-63.
549 **Mahdi LK, Miyauchi S, Uhlmann C, Garrido-Oter R, Langen G, Wawra S, Niu Y, Guan**
550 **R, Robertson-Albertyn S, Bulgarelli D, et al. 2022.** The fungal root endophyte
551 Serendipita vermifera displays inter-kingdom synergistic beneficial effects with the
552 microbiota in Arabidopsis thaliana and barley. *The ISME Journal* **16**(3): 876-889.
553 **Martin F, Tan H. 2025.** Saprotrophy-to-symbiosis continuum in fungi. *Current Biology*
554 **35**(11): R469-R475.
555 **Martínez-Cruz J, Romero D, Hierrezuelo J, Thon M, de Vicente A, Pérez-García A.**
556 **2021.** Effectors with chitinase activity (EWCAs), a family of conserved, secreted
557 fungal chitinases that suppress chitin-triggered immunity. *The Plant Cell* **33**(4):
558 1319-1340.
559 **Matroodi S, Motallebi M, Zamani M, Moradyar M. 2013.** Designing a new chitinase with
560 more chitin binding and antifungal activity. *World J Microbiol Biotechnol* **29**(8):
561 1517-1523.
562 **Mesny F, Miyauchi S, Thiergart T, Pickel B, Atanasova L, Karlsson M, Hüttel B, Barry**
563 **KW, Haridas S, Chen C, et al. 2021.** Genetic determinants of endophytism in the
564 Arabidopsis root mycobiome. *Nature Communications* **12**(1): 7227.
565 **Monge EC, Tuveng TR, Vaaje-Kolstad G, Eijsink VGH, Gardner JG. 2018.** Systems
566 analysis of the glycoside hydrolase family 18 enzymes from Cellvibrio japonicus

characterizes essential chitin degradation functions. *J Biol Chem* **293**(10): 3849-3859.

Sarkar D, Rovenich H, Jeena G, Nizam S, Tissier A, Balcke GU, Mahdi LK, Bonkowski M, Langen G, Zuccaro A. 2019. The inconspicuous gatekeeper: endophytic Serendipita vermifera acts as extended plant protection barrier in the rhizosphere. *New Phytologist* **224**(2): 886-901.

Seidl V. 2008. Chitinases of filamentous fungi: a large group of diverse proteins with multiple physiological functions. *Fungal Biology Reviews* **22**(1): 36-42.

Snelders NC, Petti GC, van den Berg GCM, Seidl MF, Thomma BPHJ. 2021. An ancient antimicrobial protein co-opted by a fungal plant pathogen for in planta mycobiome manipulation. *Proceedings of the National Academy of Sciences* **118**(49): e2110968118.

Snelders NC, Rovenich H, Petti GC, Rocafort M, van den Berg GCM, Vorholt JA, Mesters JR, Seidl MF, Nijland R, Thomma BPHJ. 2020. Microbiome manipulation by a soil-borne fungal plant pathogen using effector proteins. *Nature Plants* **6**(11): 1365-1374.

Stergiopoulos I, de Wit PJGM. 2009. Fungal Effector Proteins. *Annual Review of Phytopathology* **47**(Volume 47, 2009): 233-263.

Tsujibo H, Kubota T, Yamamoto M, Miyamoto K, Inamori Y. 2003. Characterization of Chitinase Genes from an Alkaliphilic Actinomycete, Nocardiopsis prasina OPC-131. *Applied and Environmental Microbiology* **69**(2): 894-900.

Vaaje-Kolstad G, Tuveng TR, Mekasha S, Eijsink VGH 2019. Enzymes for Modification of Chitin and Chitosan. *Chitin and Chitosan*, 189-228.

van Aalten DM, Komander D, Synstad B, Gåseidnes S, Peter MG, Eijsink VG. 2001. Structural insights into the catalytic mechanism of a family 18 exo-chitinase. *Proc Natl Acad Sci U S A* **98**(16): 8979-8984.

Vandenkoornhuyse P, Baldauf SL, Leyval C, Straczek J, Young JPW. 2002. Extensive Fungal Diversity in Plant Roots. *Science* **295**(5562): 2051-2051.

Wawra S, Fesel P, Widmer H, Neumann U, Lahrmann U, Becker S, Hehemann J-H, Langen G, Zuccaro A. 2019. FGB1 and WSC3 are in planta-induced β-glucan-binding fungal lectins with different functions. *New Phytologist* **222**(3): 1493-1506.

Wawra S, Fesel P, Widmer H, Timm M, Seibel J, Leson L, Kesseler L, Nostadt R, Hilbert M, Langen G, et al. 2016. The fungal-specific β-glucan-binding lectin FGB1 alters cell-wall composition and suppresses glucan-triggered immunity in plants. *Nature Communications* **7**(1): 13188.

Yang C, Yu Y. 2019. Binding of the Magnaporthe oryzae Chitinase MoChia1 by a Rice Tetratricopeptide Repeat Protein Allows Free Chitin to Trigger Immune Responses. **31**(1): 172-188.

Zhang Y, Yang Z, Yang Y, Han A, Rehneke L, Ding L, Wei Y, Liu Z, Meng Y, Schäfer P, et al. 2024. A symbiont fungal effector relocalizes a plastidic oxidoreductase to nuclei to induce resistance to pathogens and salt stress. *Current Biology* **34**(13): 2957-2971.e2958.

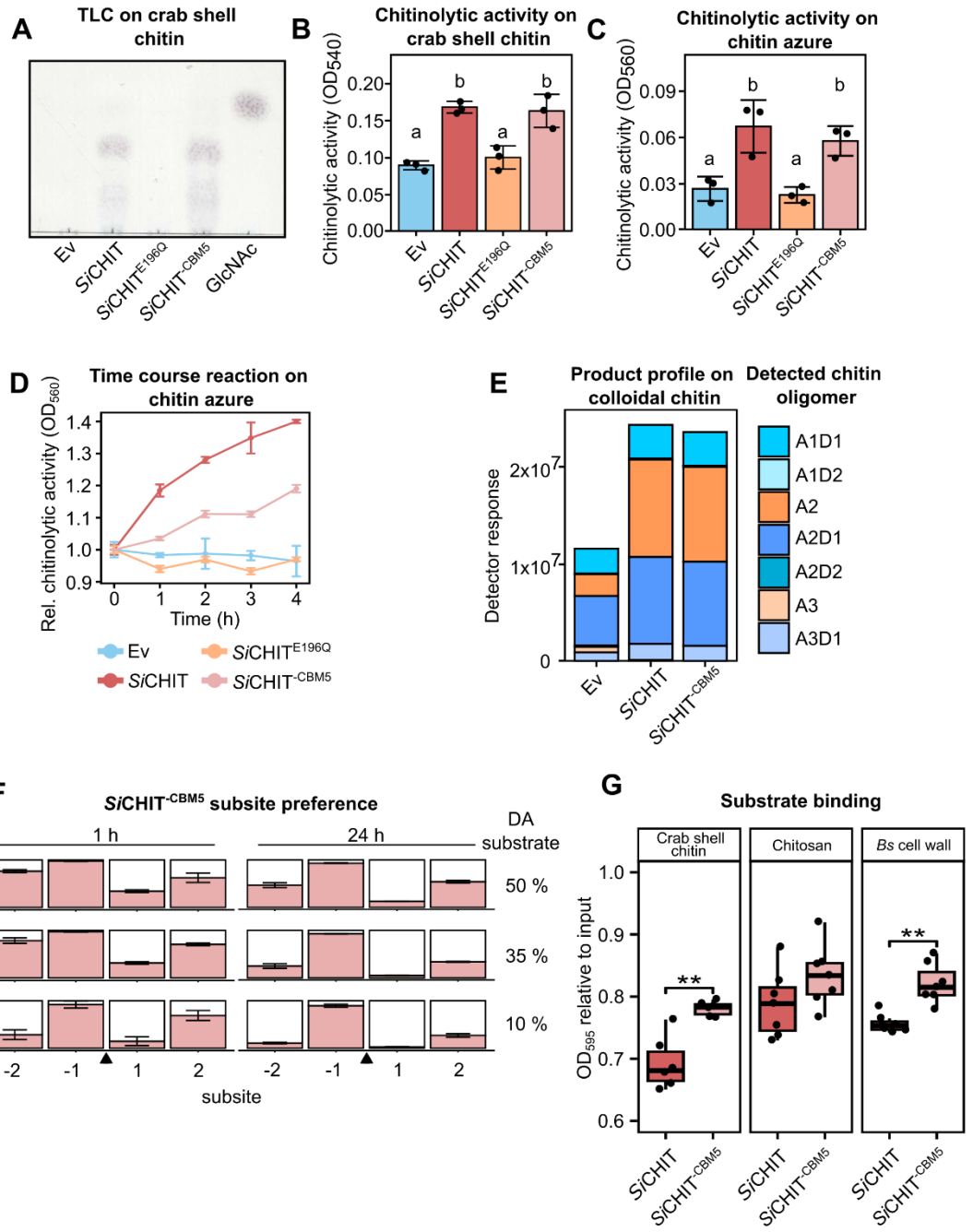

Figure 1: CBM5 enhances binding to fungal cell wall and crystalline chitin and promotes hydrolysis without affecting product specificity. A) Thin layer chromatography (TLC) of crab shell chitin incubated with the Ev control or 10 µM of *Si*CHIT, *Si*CHIT^{E196Q}, or *Si*CHIT^{-CBM5} at 28 °C for 20 h. **B)** Chitinase activity of recombinant chitinases on crab shell chitin at 10 µM and after 20 h at 28 °C. Samples were spun down and supernatants mixed 1:1 with DNSA reagent. Samples were incubated at 100 °C for 10 min and placed on ice. Subsequently, the relative amount of reducing ends was measured at 540 nm (mean +/- SD, n = 3). **C)** Chitinase activity of recombinant chitinases at 10 µM after 20 h at 28 °C on chitin azure (CA). Samples were spun down and supernatants were quantified at 560 nm (mean +/- SD, n = 3). **D)** Chitinase activity of recombinant chitinases at 10 µM measured over 4 h at 28 °C and normalized to the value of t_0 (mean +/- SEM, n = 3). **E)** Product profile of *Si*CHIT and *Si*CHIT^{-CBM} on colloidal chitin. Samples were incubated with

5 µM of chitinases for 24 h at 28 °C and hydrolysis products were identified and quantified via MS. A = acetylated, D = de-acetylated unit. **F)** Subsite preference of *Si*CHIT^{-CBM5} measured by MS. Chitosan of three degrees of acetylation (DA) were hydrolyzed for 1 h or 24 h. Based on the sequenced products, the frequency of acetylated units at the -2 to +2 subsites of *Si*CHIT^{-CBM5} was determined. The black arrow indicates the gylcosidic bond between the -1 and +1 subsite that is cleaved by the enzyme. **G)** Substrate-binding ability of *Si*CHIT and *Si*CHIT^{-CBM5} on crab shell chitin, > 75 % de-acetylated chitosan or lyophilized *Bs* mycelium. Binding was assessed by measuring the protein amount in the supernatant of reactions compared to input amount (n = 6-8). Limits of the boxplots represent the 25th–75th percentile, the horizontal line represents the median and the whiskers the minimum/maximum values without outliers. Statistical analysis: **B** and **D)** Different letters indicate significant differences according to one-way ANOVA followed by Tukey's HSD test (adjusted p-value < 0.05). **G)** Student's t-test (P-value: * < 0.05; ** < 0.01).

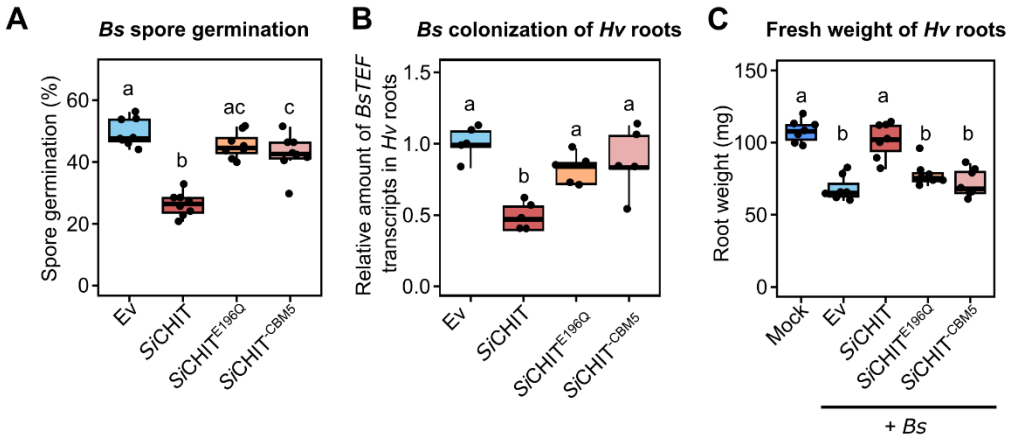

Figure 2: The CBM5 domain is essential for the antifungal and plant-protective activity of SiCHIT. A) Relative *Bs* spore germination six h post incubation in sterile chamber slides with the Ev control or 10 µM of *Si*CHIT, *Si*CHIT^{E196Q} or *Si*CHIT^{-CBM5} (n = 6). **B)** Colonization of *Hv* roots by *Bs* at three dpi inferred from relative expression of the fungal housekeeping gene *BsTEF* compared to the *Hv* housekeeping gene *HvUBI* inferred by qPCR using the $2^{-\Delta CT}$ method. Colonization values were normalized to the Ev control. *Bs* spores were either pre-treated with the Ev control or 10 µM of recombinant chitinases for 20 h at 28 °C (mean +/- SD, n = 4). **C)** *Hv* root fresh weight at three dpi with *Bs* spores. *Bs* spores were either pre-treated with the Ev control or 10 µM of recombinant chitinases for 20 h at 28 °C (n = 5-7). Limits of the boxplots represent the 25th–75th percentile, the horizontal line represents the median and the whiskers the minimum/maximum values without outliers. Statistical analysis: Different letters indicate significant differences according to one-way ANOVA followed by Tukey's HSD test (adjusted p-value < 0.05).

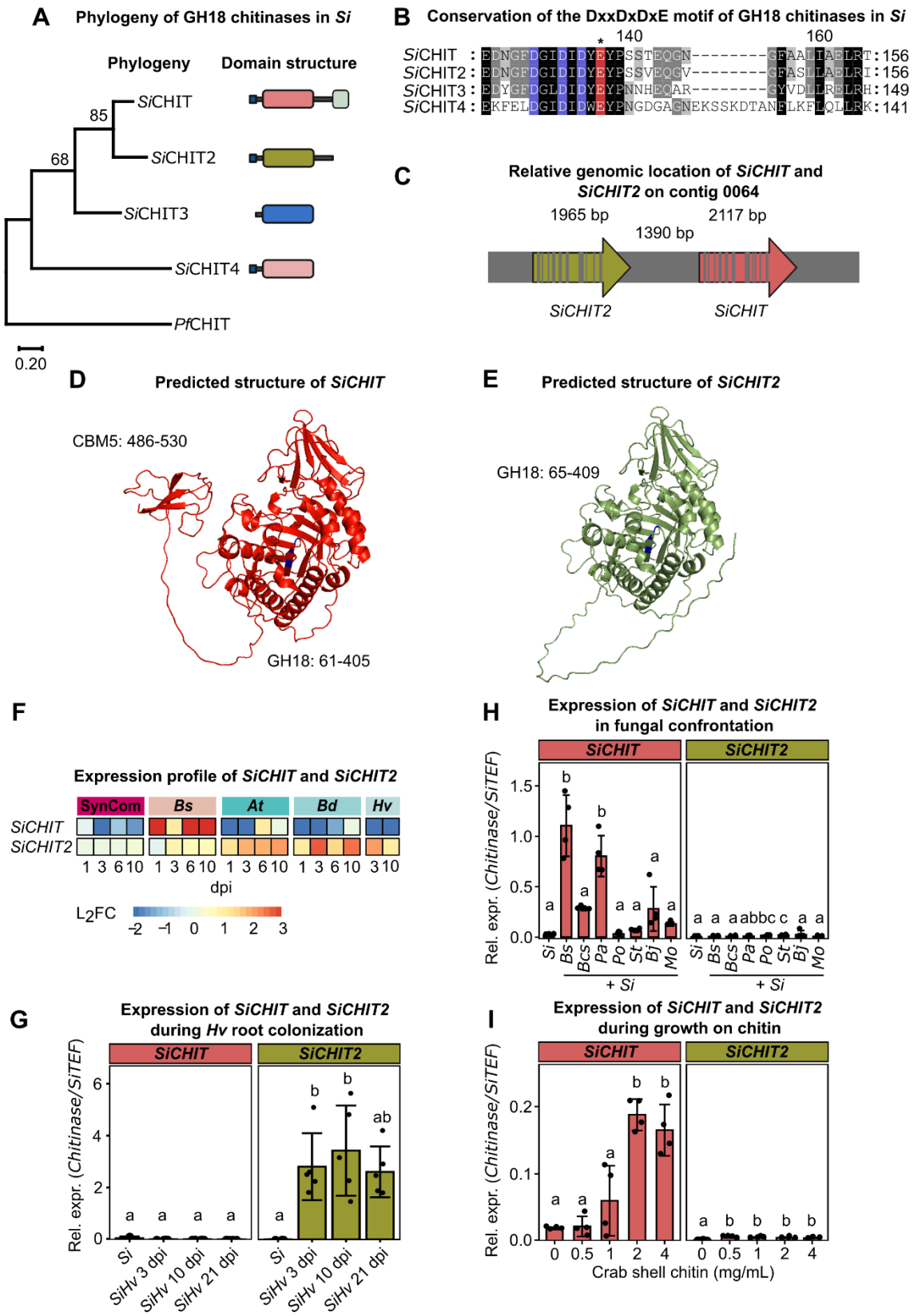
A
Phylogeny of GH18 chitinases in Si
Phylogeny
Domain structure
SiCHIT
SiCHIT2
SiCHIT3
SiCHIT4
PfCHIT
85
68
0.20
B
Conservation of the DxxDxDxE motif of GH18 chitinases in Si
140
160
SiCHIT : EDNGFDGIDIDYEYPSSTEQGN--------GFAALIAELRT:156
SiCHIT2 : EDNGFDGIDIDYEYPSSVEQGV--------GFASLLAELRI:156
SiCHIT3 : EDYGFDGLDIDYEYPNNHEQAR--------GYVDLLRELRH:149
SiCHIT4 : EKFELDGIDIDWEYPNGDGACNEKSSKDTANELKFLQLLRK:141
C
Relative genomic location of SiCHIT and SiCHIT2 on contig 0064
1965 bp
1390 bp
2117 bp
SiCHIT2
SiCHIT
D
Predicted structure of SiCHIT
CBM5: 486-530
GH18: 61-405
E
Predicted structure of SiCHIT2
GH18: 65-409
F
Expression profile of SiCHIT and SiCHIT2
SynCom
Bs
At
Bd
Hv
SiCHIT
SiCHIT2
1 3 6 10
dpi
L2FC
-2 -1 0 1 2 3
G
Expression of SiCHIT and SiCHIT2 during Hv root colonization
SiCHIT
SiCHIT2
Rel. expr. (Chitinase/SiTEF)
Si
SiHv 3 dpi
SiHv 10 dpi
SiHv 21 dpi
H
Expression of SiCHIT and SiCHIT2 in fungal confrontation
SiCHIT
SiCHIT2
Rel. expr. (Chitinase/SiTEF)
Si
Bs
Bcs
Pa
Po
St
Bj
Mo
+ Si
I
Expression of SiCHIT and SiCHIT2 during growth on chitin
SiCHIT
SiCHIT2
Rel. expr. (Chitinase/SiTEF)
0 0.5 1 2 4
Crab shell chitin (mg/mL)

Figure 3: *SiCHIT2* encodes a GH18 chitinase without CBM5 and is expressed during host plant colonization. A) Maximum likelihood tree of all four GH18 chitinases encoded by *Si*. Signal peptides were predicted by SignalP 5.0 and removed prior to amino acid sequence alignment. Amino acid sequences were aligned using the MUSCLE algorithm. A maximum likelihood tree was constructed with 500 bootstraps. A GH18 chitinase from *Plasmodium falciparum* was used as outgroup. Symbols on the right indicate the domain architecture of the full length proteins: small blue box: signal peptide; grey line: inter-domain regions; larger boxes (red, green, blue, beige): GH18 domain; small green box in *Si*CHIT: CBM5. **B)** Amino acid sequence alignment of the catalytic DxxDxDxE motif. Blue: conserved aspartate (D); red: conserved glutamate (E). The asterisk indicates the glutamate that was mutated to glutamin (Q) in the catalytically inactive *Si*CHIT^{E196Q}. **C)** Scheme of the relative location of *SiCHIT* and *SiCHIT2* in the genome of *Si* on contig 0064. The grey bars illustrate introns. *SiCHIT* has 11, and *SiCHIT2* 10 introns. **D, E)** Structure prediction of *Si*CHIT and *Si*CHIT2 by AlphaFold. The sequences of predicted signal peptides were identified with SignalP 5.0 and removed prior to structure prediction. **F)** Expression profile of *SiCHIT* and *SiCHIT2* during confrontation with a bacterial community (SynCom), the pathogen *B. sorokiniana* (*Bs*), or during colonization of the host plants *A. thaliana* (*At*), *B. distachyon* (*Bd*) or *H. vulgare* (*Hv*). The data was taken from Eichfeld *et al.* 2024. **G)** Expression of *SiCHIT* or *SiCHIT2* during *Hv* root colonization at 3, 10 and 21 dpi. Four day old *Hv* roots were inoculated with *Si* and grown on 1/10 PNM medium. Expression was inferred by relative expression of the fungal housekeeping gene *SiTEF* compared to *SiCHIT* or *SiCHIT2* by qPCR using the $2^{-\Delta CT}$ method (mean +/- SD, n = 3-5). **H)** Expression of *SiCHIT* or *SiCHIT2* at six days of growth on 1/10 PNM medium with different fungal species (*Bs* = *Bipolaris sorokiniana*; *Bcs* = *Brunneochlamydosporium sp.*; *Pa* = *Papulaspora equi*; *Po* = *Podospora sp.*; *St* = *Stachybotrys sp.*; *Bj*: *Bjerkandera sp.*; *Mo* = *Mortierella sp.*. Fungal liquid cultures were grown in CM and washed with water, mixed in a 1:1 ratio and 1 g mycelium was streaked out on plates. Expression was inferred by relative expression of the fungal housekeeping gene *SiTEF* compared to *SiCHIT* or *SiCHIT2* by qPCR using the $2^{-\Delta CT}$ method (mean +/- SD, n = 4). **I)** Expression of *SiCHIT* or *SiCHIT2* at six days of growth on crab shell chitin-containing PNM medium at different concentrations. *Si* liquid culture grown in CM was washed with water and 1 g mycelium was streaked out on 1/10 PNM plates. Expression was inferred by relative expression of the fungal housekeeping gene *SiTEF* compared to *SiCHIT* or *SiCHIT2* by qPCR using the $2^{-\Delta CT}$ method (n = 4). Statistical analysis: Statistical analysis: Different letters indicate significant differences according to one-way ANOVA followed by Tukey's HSD test (adjusted p-value < 0.05).

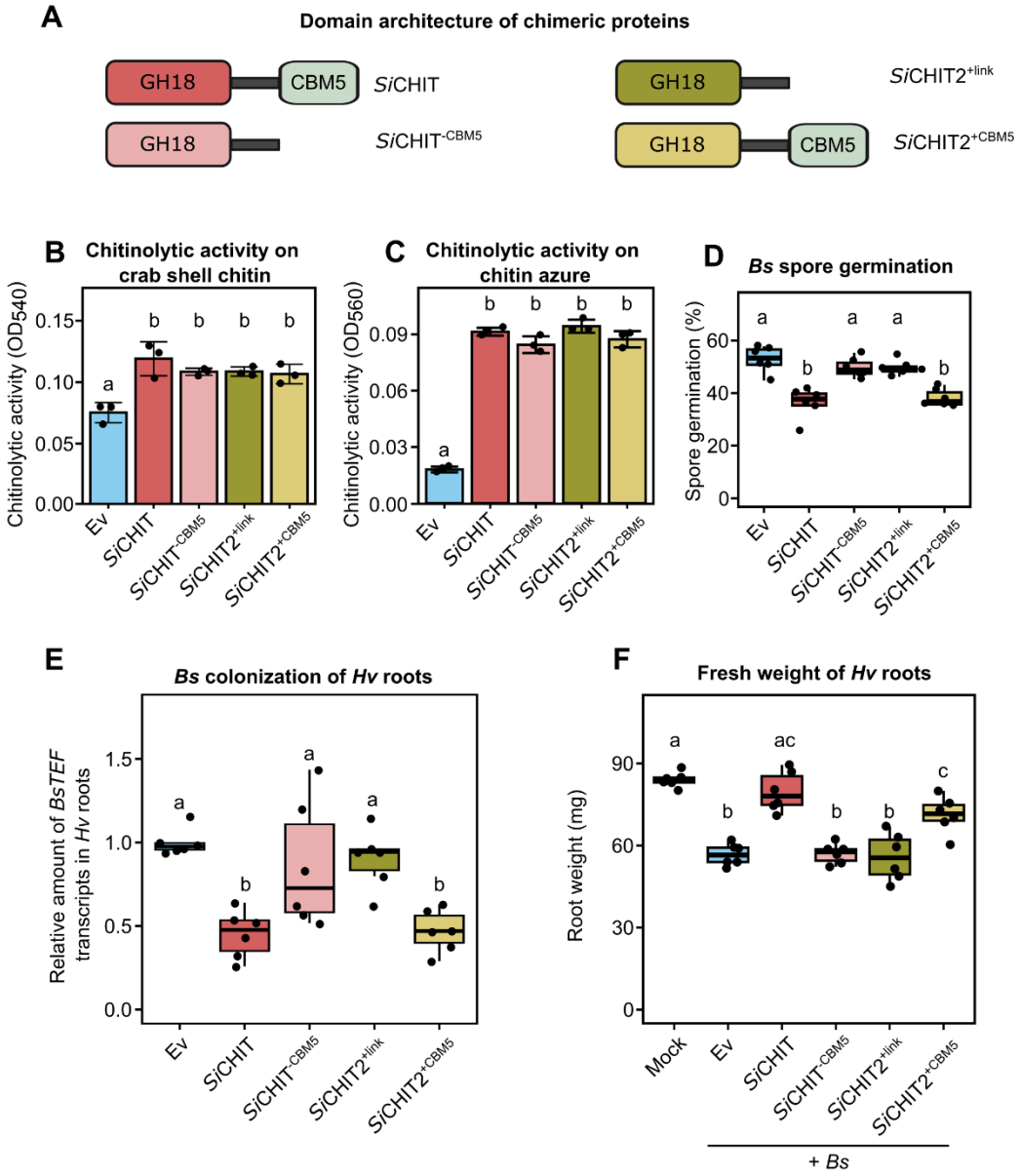

Figure 4: Fusion of the CBM5 to *Si*CHIT2 activates its antifungal and plant-protective capacity. A) Domain architecture of recombinant proteins. *Si*CHIT2^{+link} contains the GH18 domain of *Si*CHIT2 and the linker region of *Si*CHIT. *Si*CHIT2^{+CBM5} contains the GH18 domain of *Si*CHIT2 and the linker region with the CBM5 of *Si*CHIT. **B)** Chitinase activity of recombinant chitinases on crab shell chitin at 10 µM and after 20 h at 28 °C. Samples were spun down and supernatants mixed 1:1 with DNSA reagent. Samples were incubated at 100 °C for 10 min and placed on ice. Subsequently, the relative amount of reducing ends was measured at 540 nm (mean +/- SD, n = 3). **C)** Chitinase activity of recombinant chitinases at 10 µM after 20 h at 28 °C on chitin azure (CA). Samples were spun down and supernatants were quantified at 560 nm (mean +/- SD, n = 3). **D)** Relative *Bs* spore germination six h post incubation in sterile chamber slides with Ev control or 10 µM of *Si*CHIT, *Si*CHIT^{-CBM5}, *Si*CHIT2^{+link} or *Si*CHIT^{+CBM5}. (n = 6). **E)** Colonization of *Hv* roots by *Bs* at three dpi inferred from relative expression of the fungal housekeeping gene *BsTEF* compared to the *Hv* housekeeping gene *HvUBI* by qPCR using the $2^{-\Delta CT}$ method. Colonization values were normalized to the Ev control. *Bs* spores were either pre-treated with the Ev control or 10 µM of recombinant chitinases for 20 h at 28 °C (n = 6). **F)** *Hv* root fresh weight at three dpi with *Bs* spores. *Bs* spores were either pre-

treated with the Ev control or 10 µM of recombinant chitinases for 20 h at 28 °C. Limits of the boxplots represent the 25th–75th percentile, the horizontal line represents the median and the whiskers the minimum/maximum values without outliers (n = 6). Statistical analysis: Different letters indicate significant differences according to one-way ANOVA followed by Tukey's HSD test (adjusted p-value < 0.05).

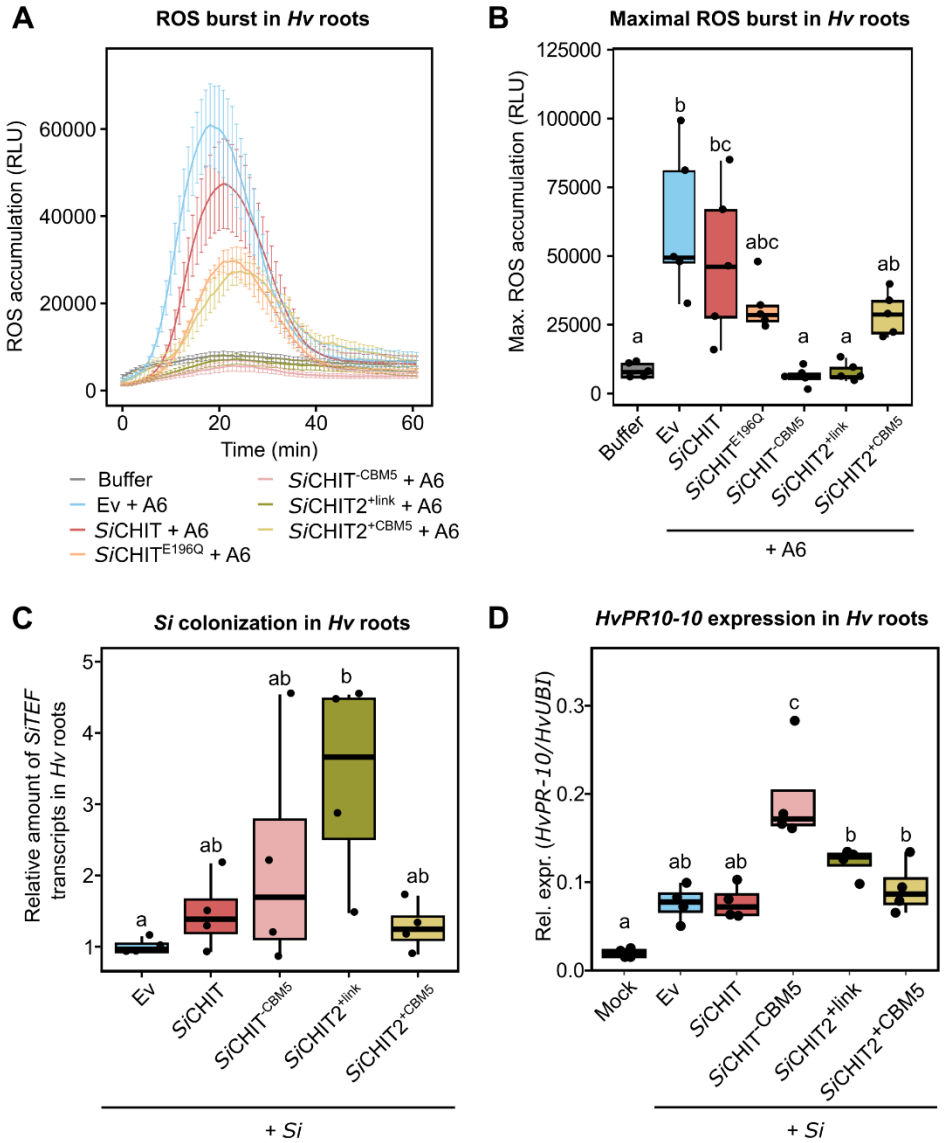

Figure 5: *Si*CHIT2 suppresses chitin-triggered immunity and facilitates root colonization by *Si* in *Hv*. A) ROS burst of 4 d *Hv* roots after treatment with 125 nM chitohexaose (A6). Chitohexaose was incubated with the indicated recombinant chitinases in an equimolar concentration (10 µM) 20 h prior to treatment of *Hv* roots. Values represent means +/- SD from five to six individual wells containing four root pieces of ~ 0.5 cm. **B)** Maximum values of ROS accumulation of *Hv* roots (data from **A**). **C)** Colonization of *Hv* roots by *Si* at three dpi inferred from relative expression of the fungal housekeeping gene *SiTEF* compared to the *Hv* housekeeping gene *HvUBI* by qPCR using the $2^{-\Delta CT}$ method. Colonization values were normalized to the Ev control. *Si* spores were germinated for 16 h at 28 °C and either incubated with the Ev control or 20 µM of recombinant chitinases immediately before *Hv* root inoculation (n = 4). **D)** Transcript accumulation of the *Hv* defense marker gene *Hv*PR10 at three dpi inferred by relative expression of *HvPR10* relative to the *Hv*

housekeeping gene *HvUBI* by qPCR using the $2^{-\Delta CT}$ method (n = 4). Limits of the boxplots represent the 25th–75th percentile, the horizontal line represents the median and the whiskers the minimum/maximum values without outliers. Statistical analysis: Different letters indicate significant differences according to one-way ANOVA followed by Tukey's HSD (adjusted p-value < 0.05).

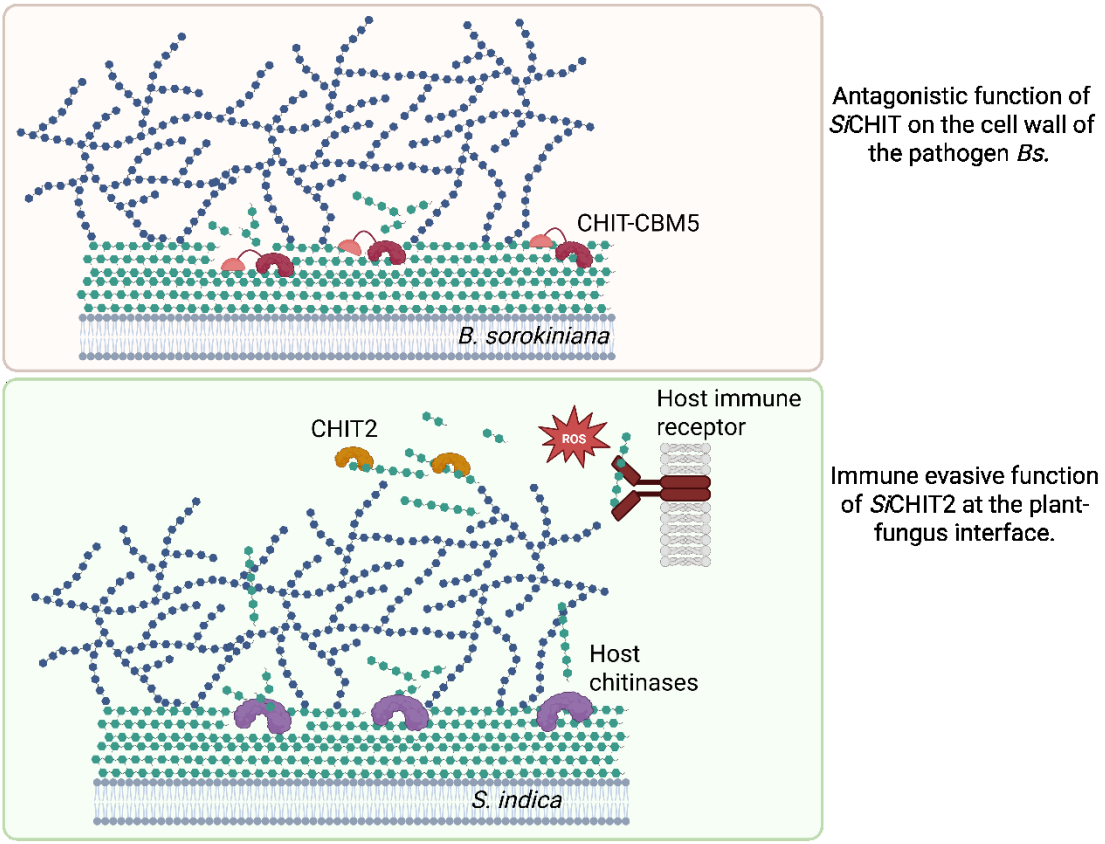

Figure 6: Model displaying the divergent functions of *Si*CHIT and *Si*CHIT2. During confrontation with the pathogen *Bs*, *Si* secretes a GH18-CBM5 chitinase that efficiently inhibits the growth of *Bs*, enabling *Si* to secure its ecological niche. To effectively function in this context, *Si*CHIT relies on the presence of the CBM5. The paralogous *Si*CHIT2 has a catalytically active GH18 domain but no CBM5. It serves *Si* during host colonization by preventing the elicitation of chitin-triggered immunity at the fungus-plant interface, putatively by degrading immunogenic chitin oligomers that are released from the cell wall of *Si* by host chitinases. Figure was created using Biorender.